Separation Science and Technology

ISSN: 0149-6395 (Print) 1520-5754 (Online) Journal homepage: http://www.tandfonline.com/loi/lsst20

Effect of operating parameters on fine particle grinding in a vertically stirred media mill

Yang Yang, Neil A. Rowson, Richard Tamblyn & Andy Ingram

To cite this article: Yang Yang, Neil A. Rowson, Richard Tamblyn & Andy Ingram (2017) Effect of operating parameters on fine particle grinding in a vertically stirred media mill, Separation Science and Technology, 52:6, 1143-1152, DOI: 10.1080/01496395.2016.1276931

To link to this article: http://dx.doi.org/10.1080/01496395.2016.1276931

Accepted author version posted online: 10 Jan 2017.
Published online: 10 Jan 2017.

SEPARATION SCIENCE AND TECHNOLOGY
2017, VOL. 52, NO. 6, 1143–1152
http://dx.doi.org/10.1080/01496395.2016.1276931

Taylor & Francis
Taylor & Francis Group

Effect of operating parameters on fine particle grinding in a vertically stirred media mill

Yang Yang[a], Neil A. Rowson[a], Richard Tamblyn[b], and Andy Ingram[a]

[a]School of Chemical Engineering, University of Birmingham, Edgbaston, Birmingham, UK; [b]IMERYS, Par Moor Centre, Par, Cornwall, UK

ABSTRACT

This article evaluates the effects of operating parameters on fine particle grinding process with a vertically stirred media mill. The effects are investigated through size reduction under different operating conditions by changing solids content, tip speed and the configuration of the impeller. Solids content at 65% (w/w) is demonstrated to be more efficient than 75% (w/w). The maximum difference in product size (D_{80}) is about 2 μm. Velocity maps are described at tip speeds of 5.23 m/s, 6.54 m/s and 9.81 m/s by positron emission particle tracking (PEPT). The lower tip speed saves the specific energy 50–100 kWh/t. Over energy input 100–300 kWh/t, D_{80} of product is reduced 1–2μm by replacing standard impeller with new types of impeller.

ARTICLE HISTORY
Received 1 September 2016
Accepted 22 December 2016

KEYWORDS
Comminution; fine particle grinding; PEPT; stirred media mill

Introduction

Due to higher energy efficiency and the ability to produce the extremely fine size of the product, stirred media mills are frequently used to grind fine or ultra-fine particles in many industrial applications such as pharmaceutical, cosmetic, paints and paper manufacture.[1–4] Compared to the traditional tumbling ball mills, stirred media mills use an agitator to mix the feeding material and the grinding beads. Instead of the impact force, the shear force caused by the attrition is the main breakage mechanism for stirred media mills. When the required particle size is down to several microns (e.g. $D_{80} \leq 10\mu m$), stirred media mills demonstrate significant improvements in energy saving over tumbling ball mills.[5,6] This is attributed to using the small size media at higher media loading stirred at higher speed of impeller, which may be as high as $20m/s$.[7] Thus, energy intensity is improved greatly by using stirred media mill.

At these conditions, the grinding media gains higher kinetic energy and grinds the particles more efficiently when compared to the conventional milling techniques. The interactions between the particle–particle and particle–grinding bead absorb a large amount of energy transferred from the agitator, and most of the energy is dissipated as heat. Approximately 3–5% of the total input energy is actually used for effective grinding.[8] In the last decades, some research has identified that the grinding efficiency is influenced by some important technical parameters such as specific energy, tip speed, grinding media, design of grinder, impeller geometries and solid mass concentration.[1,9–11] Also, some research investigated some other factors such as process methods (e.g. circulated process) and size of grinding mill.[12,13] As milling is inherently an inefficient process, the influence of these factors is still not fully understood.

Hence, this study was focused to analyse the performance of vertically stirred media mills through investigating particle size reduction, flow pattern by varying the operating parameters of solids loading, specific energy utilizations, tip speed, grinding media and configuration of the impellers, because these parameters are believed to be the most important factors affecting the grinding performance.

Materials and methods

Experimental set-up

Within the scope, GCC(grinding calcium carbonate) was used as feed material, it is the main product of IMERYS(formerly known as English China Clay PLC) and is commonly used as a paper filler. The dry GCC powder (initial $D_{80} = 62.8\mu m$) is mixed with water to form a slurry mixture. Two types of ceramic beads were used as grinding media in the study. Carbolite was supplied by CARBO ceramic grinding media company. The Carbolite media size is +0.8 to −1.2 mm with an apparent specific gravity 2.7 ± 0.1. The other was

CONTACT Yang Yang yangy30685@live.co.uk School of Chemical Engineering, University of Birmingham, Edgbaston, Birmingham, B15 2TT, UK.
Color versions of one or more of the figures in the article can be found online at www.tandfonline.com/lsst.

ZirPro, a zirconium-based material supplied by Saint-Gobain. The media size range is +0.7 to −1.4 mm, with an apparent specific gravity 3.2 ± 01. Carbolite is slightly finer and lighter than ZirPro, but surface is not as smooth as ZirPro (Fig. 1). The media filling ratio for both types of grinding media was kept at 52% (volume of media/volume of media and slurry) for all tests.

Figure 2 displays the set-up for the lab-scale grinding mill supplied by IMERYS. The mill consists of a grinding pot (V = 2.9L), a digital controller for changing rotation speed and a vertically mounted impeller driven by a motor (Fig. 2a). A central pin-type impeller with two sets of 90° offset pin is used as a standard configuration (Fig. 2b). Some other configurations of the impeller that were tested in the experimental programme are explained in the Results section. The mill chamber is made of polyethylene, and no wear liner is applied. The energy drawn by the mill is measured by a torque sensor located under the bottom of the mill chamber. The recorded torque force is converted into the corresponding power. The energy input is calculated by integration of the power over the grinding time.

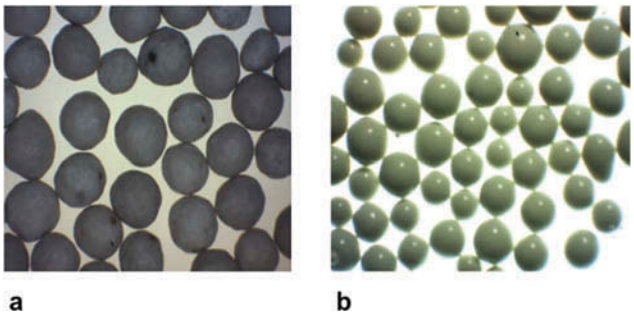

Figure 1. Photographs of the grinding media used in the tests (a) Carbolite and (b) ZirPro.

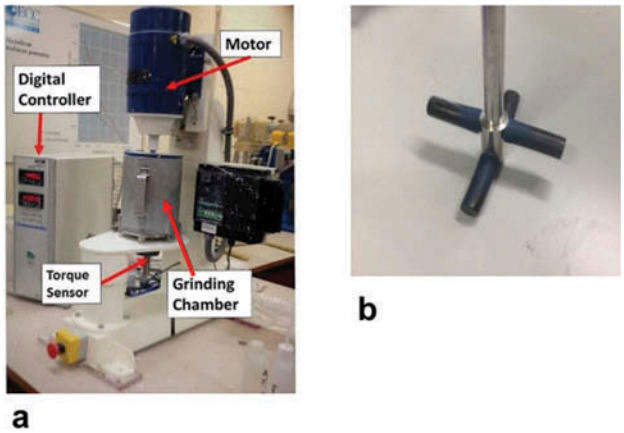

Figure 2. Experimental set-up for the lab-scale mill (a) and the standard impeller (b).

Figure 3 depicts the dimensions of the grinding chamber, and it indicates the relative position of the impellers inside the grinding pot. The cross-sectional shape of the pot is a circle with a diameter D = 140mm. The height (H) of the grinding pot is 190mm with a cover of which thickness can be ignored; hence, the aspect ratio d/h is 14 : 19(0.736). The diameter of the impeller d is 125mm. Thus, the gap(w) between the tip of stirrer and wall of the chamber is 7.5mm. Compared to the diameter of the stirrer(d), the gap is quite narrow. The breakage of the particles is believed to be mainly occurred within this gap, as the tip of stirrer produces large velocity gradient against to the wall chamber.

The feed slurry is prepared by dispersing ground calcium carbonate in water at 65% and 75% w/w two level of solids concentration defined as (1) follows:

$$\varphi = \frac{m_{CaCo_3}}{m_{CaCo_3} + m_{water}} \quad (1)$$

The density of ground calcium carbonate is 2700kg · m^{-3} according to the supplier. The size distributions of the samples were measured by Mastersizer (Malvern Instruments, UK) laser diffraction particle size analyzer

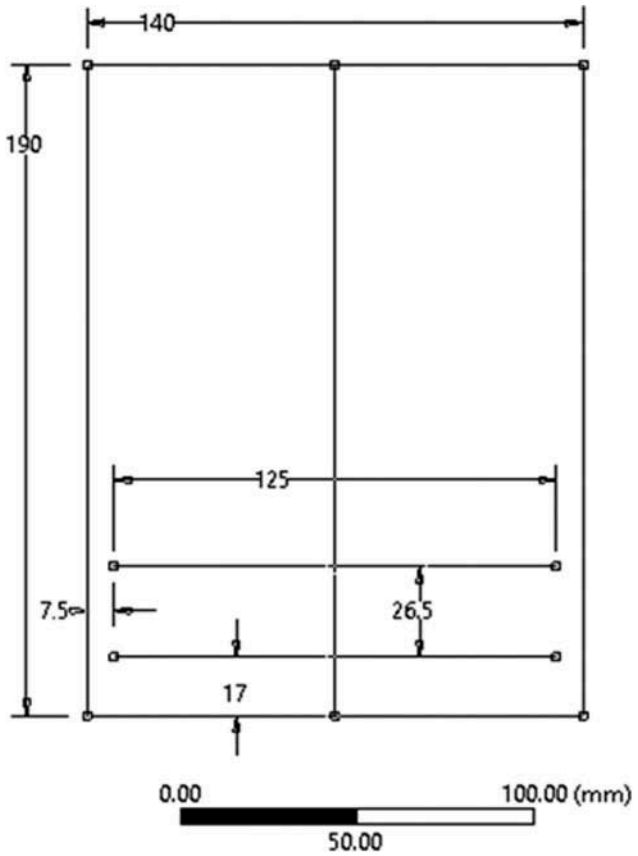

Figure 3. Geometry layout of the grinding chamber for the lab-scale mill.

found at University of Birmingham, UK. The powerP(W) drawn by the mill was calculated from the recorded torque force by Eqs. (2) and (3):

$$P = T \cdot \omega \tag{2}$$

$$\omega = \frac{2\pi \cdot N}{60} \tag{3}$$

where T(Nm) is torque force, $\omega(\mathrm{rad} \cdot \mathrm{s}^{-1})$ is angular velocity, and N(rpm) is revolution speed.

Positron emission particle tracking

Many visualization methods have been applied for plotting the velocity map and describing the flow behavior in a stirred media mill. The common methods such as particle image velocimetry (PIV) and laser Doppler anemometry (LDA) are applied in modelling dilute suspension.[14,15] By using the laser technology, these optical methods require the investigated samples and vessel to be transparent. Hence, it is not suitable for the high solids content where the laser light is nearly all absorbed by the slurry. Another limitation is that the laser light cannot pass through the vessel made of the metal. Normally, the grinding chamber is made of metal material such as steel or aluminium with a polymer wear liner. Magnetic resonance imaging(MRI) has been successfully applied to identify the velocity distribution in many cases even with high viscous slurry or multi-phase mixing process, but it is rarely used with metal equipment.[14]

Positron emission particle tracking (PEPT) developed by University of Birmingham is an ideal method for the study of high solids concentration slurry within opaque grinding chamber (Fig. 4). PEPT was firstly used for medical purpose. Recently, it was introduced and applied to explore mixing processes in a stirred tank.[16] Compared with PIV or LDA, PEPT uses $\gamma -$ ray, which overcomes the requirement of the samples to be transparent. As gamma-rays are quite penetrating for metal (50% are transmitted through 11-mm steel), it is able to measure velocity distribution of materials inside metal vessels.

PEPT identifies the sample local velocity by tracking a radioactive tracer in the system. Normally, the tracer could be a glass or ceramic bead with size down to 1mm. In this study, a grinding bead is directly irradiated to be the tracer. Hence, the trace shows no physical difference with other grinding media. The recorded velocity of the tracer then represents the velocity of flow at this specific spatial position and time point as the tracer faithfully follows the flow dynamic and moves inside the system. The radioactive tracer continues releasing γ-rays when a positron annihilates with an electron. These γ-rays are detected by two separate stationary positron cameras.[17] By collecting a larger number of γ-rays, the tracer trajectory is reconstructed in 3-D coordinates. The path of the tracer is recorded against real time, so the local instantaneous velocity is easily calculated. Some gamma-rays may be scattered prior detection causing an error at locating tracer positions. It is possible to provide estimated of its instantaneous velocity accurate to 10%.

Figure 4. The grinding mill is examined by the PEPT.[25]

Results and discussion

Morphology of calcium carbonate

Figure 5a displays a photograph taken by scanning electron microscopy for the feed material with 100 μm length scale. It can be clearly seen that the shape of most particles is non-spherical. It undoubtedly increases the complexity of the size analysis because normally it requires length and width measures to describe size of a non-spherical particle. Thus, it is reasonable to assume that all particles are sphere by assigning an equivalent spherical diameter. This assumption greatly improves the efficiency of analysis, and it shows no obvious influence on the evaluation of

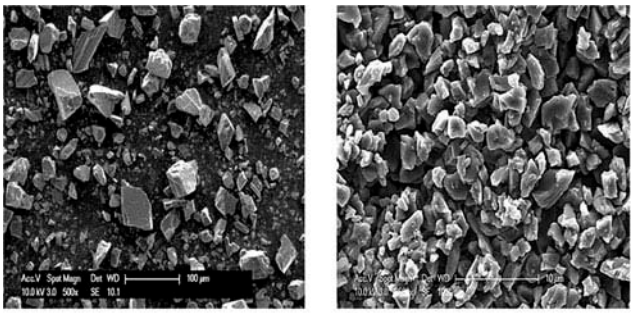

Figure 5. Photographs of the calcium carbonate particles taken by SEM (a) the feeding sample and (b) the product at 100 kWh/t energy input.

particle finesse. Also, it is essential for size measurement based on laser diffraction technology.

Figure 5b shows product size distribution at energy input 100 kWh/t. The length scale is 10 μm. Obviously, the product is much finer than the feed sample. The outline shape of calcium carbonate particle remains similarly, but D_{80} is dramatically reduced from 26.9μm (feed) to 6.2μm (100 kWh/t). The specific energy input is a key parameter, which directly affects the final product size. However, at the same level of energy input, optimal grinding operation is possible to be achieved by optimising the technical parameters.

Effect of solids concentration

The solids concentration is a key parameter affecting grinding process especially when the particle size reduces to several microns. Moys[18] pointed out that high viscous slurry tends to reduce the relative velocity of media particles compared to the slurry. When two media particles approach each other, the viscous slurry fills the area between the gaps of two media particles that works as a buffer region for reducing the relative speed. It is particularly important to minimise this barrier effect in the stirred mill more than tumbling mills because the particles in stirred mills are mainly subject to shear stress, which is unlike tumbling ball where the impact force is mainly dependent on cascading of balls.[19]

The fluid dynamic viscosity is defined as (4) follows:

$$\mu = \frac{\text{shear stress}}{\text{shear rate}} \tag{4}$$

Hence, the rheology characteristic is Newtonian for constant μ. If μ is variable, the fluid is non-Newtonian. Figure 6 illustrates some characterisztion for non-Newtonian fluids. In this study, the viscosity investigated only refers to characteristic of the slurry

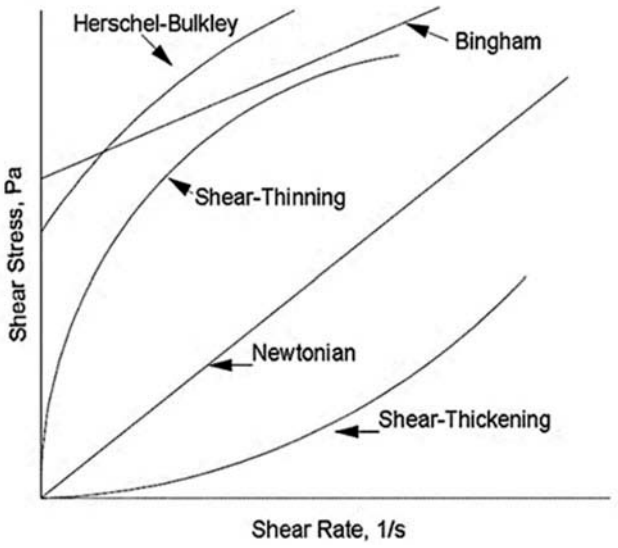

Figure 6. Shear stress versus shear rate for the time-independent non-Newtonian fluids.[26]

mixed by water and dry $CaCo_3$ powder. The interaction between the slurry and grinding beads is out of the scope of this article. The measurement was performed using an AR-2000 rheometer (TA instruments, USA).

Seen from Fig. 7, the slurry shows typical non-Newtonian characteristics (shear thinning) at both 65% and 75% solids concentration. Note that the vertical axis is a logarithm scale. Shear stress increases sharply before shear rate reaches $200s^{-1}$. Then, it gradually increases with shear rate till $800s^{-1}$. The slurry of 75% solids content always performs at a higher shear stress indicating that higher solids concentration causes greater resistance. Bernhardt et al.[20] also found a similar phenomenon on limestone slurry at 60% and 55% solids content. For many types of mineral slurry,

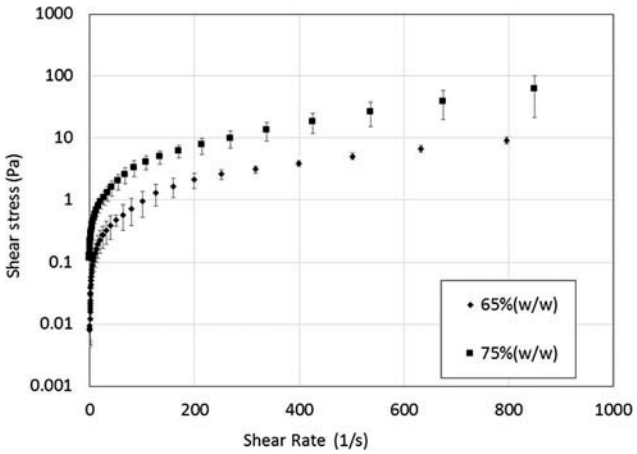

Figure 7. Shear stress (Pa) is plotted against shear rate(s^{-1}) at solids concentration 65% and 75%.

the rheology shows typical non-Newtonian characteristics particularly for high solids content.[19]

Figure 8 displays viscosity against shear rate. It clearly shows that viscosity decreases against shear rate. Overall, the slurry at 75% solids content has greater viscosity than 65% solids content. With shear rate ranges >100s^{-1}, the viscosity slightly increases for 75% solids content. Greenwood et al.[21] explain the error is caused by the sedimentation of particles in the rheometer rather than any shear-thickening phenomena. As the phenomenon is not obviously observed at 65% solids content, the effect of sedimentation is obviously less. However, for 65% solids concentration, the slurry shows nearly Newtonian phenomena over the range of shear rate >200s^{-1}. The viscosity is approximately constant at 0.01Pa.S. Obviously, lower solids loading affects less the suspension viscosity. Lower viscosity of the slurry undoubtedly means less power draw for same operating conditions in the mill.

Figure 9 displays the variation of particle size D_{80} against energy input at slurry loading 65% and 75%. The maximum difference on product size D_{80} is about 2μm. The tip speed is fixed at 6.54m/s (equivalent to 1000 rpm). The sample is tested at energy inputs of 100 kWh/t, 150 kWh/t, 200 kWh/t, 250 kWh/t and 300 kWh/t. Overall the size is clearly reduced by increasing the energy input. For the same types of grinding media, samples ground at 65% solids concentration obtain a finer product than 75% solids concentration. This indicates that the slurry with higher solids loading is harder to achieve the finer results at identical energy inputs. At the higher solids loading, it is highly possible for particles to be captured by the grinding beads, but it may not necessarily increase breakage rate. For each stress event, some of the particles are nipped between the gap area formed by two grinding bead. It is harder to break

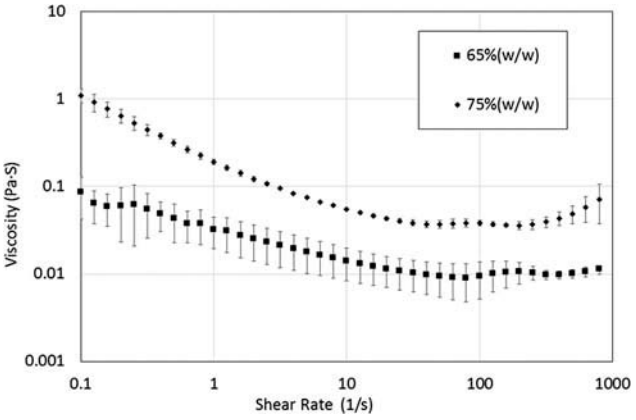

Figure 8. Viscosity (Pa·s) is plotted against shear rate (s^{-1}) at solids concentration 65% and 75%.

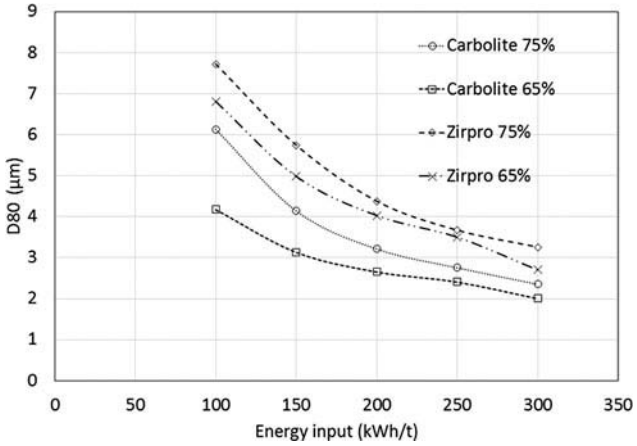

Figure 9. Details of size reduction against energy input by different solids concentration and grinding media.

couple of particles instead of a single particle or fewer under the same stress force. Hence, samples at the lower solids loading obtain finer product at either type of grinding beads. However, Ouattara and Frances[3] found a contrarily trend that higher the solids concentration, the finer particle size is obtained. In his study, samples were ground at even lower solids loading (0.3–0.05 w/w). At such low solids concentration, the probability that particle size captured by the grinding beads may play a dominant role. Increasing solids loading undoubtedly enhances the chance that particles are trapped by the grinding media. Thus, the higher solids loading may produce finer product. Therefore, optimal solids concentration is a key factor for efficiency improvement.

Effect of tip speed

Tip speed is an important operating parameter affecting the grinding results. So far, it is still difficult to draw a general conclusion for the influence of tip speed as higher tip speed may not result in finer products and vice versa. Energy intensive test studies are conducted to optimise the operating process. Some researchers investigated the effect of tip speed based on the stress intensity model to obtain the optimal operating speed for comminution process.[22,23] However, the velocity distribution within the grinding chamber is not sufficiently understood. Due to the complex physical properties of the mineral slurries, it is difficult to identify the slurry movement in the mill. Conway-Baker and colleagues[17] conducted some grinding experiments with PEPT to examine the motion of grinding media by varying some parameters such as media loading, baffles and slurry density, but the tested rotation

speed locates in a relative slow range. In this study, tip speed aims at higher values, which are more meaningful for the industrial applications.

The tests were carried out with grinding media Carbolite at tip speed 5.23m/s, 6.54m/s and 9.81m/s by fixing solids loading at 75%. Due to the symmetry, velocity map demonstrates half section of the grinding chamber. The details of velocity field are shown in Figure 10a–c. Additionally, the impeller position depicted in all figures simply indicates the field where the trajectory of the tracer particle is recorded. The vertical axis shows real size in height of grinding chamber, and the horizontal axis shows real radial distance based on the centre of the bottom. All velocity maps are calculated by programming in MATLAB (version 2014a) based on PEPT data.

As shown in Figure 10a–c, with the tip speed decreasing, the high-speed field indicated with red reduces evidently while blue indicating slow motion of charge remains almost same. The variation of velocity mainly occurred around the impeller area approximately within height band $0.02 - 0.06$m. In the surrounding area, the pattern of movement of grinding beads is not obvious. Due to high solids content (75%), grinding beads could easily clump together working as a sponge to absorb large amounts of kinetic energy transferred from the impeller. This explains why high velocity is only observed in the impeller band. Thus, even if the grinding beads give greater kinetic energy around the impeller by setting a high tip speed, it is still difficult to transfer this kinetic energy vertically to the upper area (above impeller band) or the bottom. The effective breakage of particles probably happens at the gap field between the tip of impeller and the chamber wall as the particles in this area are moving fast to impinge upon the wall resulting in abrasion and attrition with sufficient shear force for breaking particle.

In the central of the grinding chamber, the charge forms a vortex as no tracked velocity values are described near the impeller shaft. A vortex area is observed around the tip of the impeller with higher tip speed. Correspondingly, the level height of the charge increases and the packed density of the charge around the impeller tip decreases. It indicates higher tip speed may not guarantee the improvement of efficiency. In fact, the high tip speed might reduce the effective grinding area even if the particles are able to be accelerated to a higher speed. At the same time, larger radial displacement of the charge in the impeller band by applying higher tip resulted in a reduction of the effective grinding space.

In this case, the high tip speed may not improve grinding efficiency. In addition, momentum transfer between the upper area (region above the impeller) and the bottom depends greatly on the gravity. The high tip speed effects this fall back of the grinding media. Thus, it undoubtedly creates greater power intensity in the grinding chamber. If the energy is not efficiently transferred through an efficient grinding mechanism, it will mostly dissipate as the heat; hence, inefficient impact between the grinding media and the wall or impact purely between grinding media themselves consumes a large amount of energy.

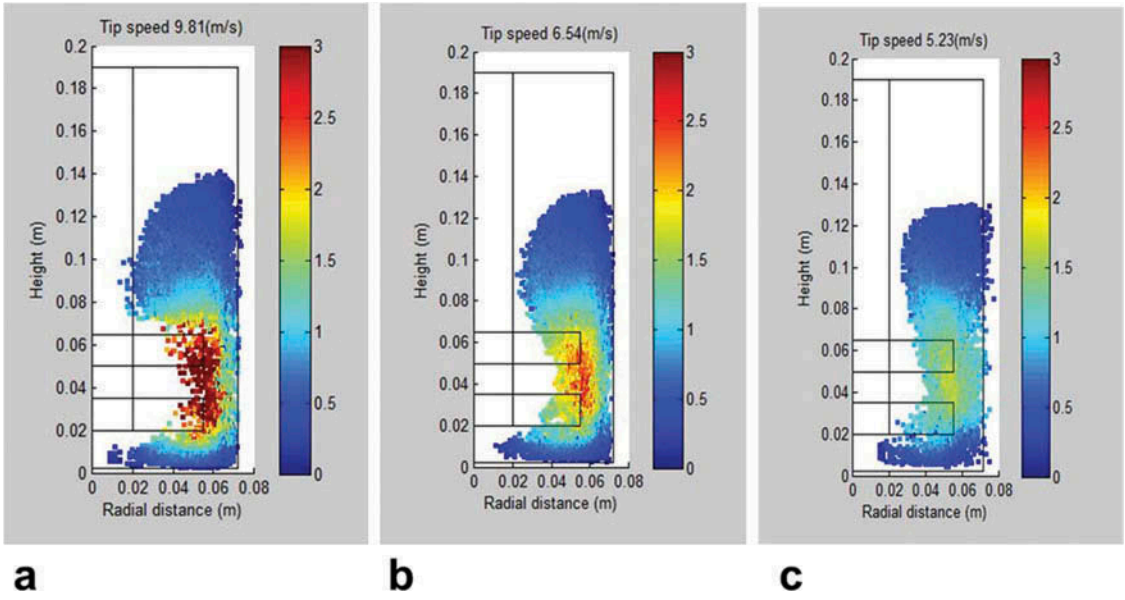

Figure 10. Velocity map with the grinding media Carbolite at the tip speed 9.81m/s (a), 6.54m/s (b) and 5.23m/s (c).

Figure 11 displays details of size variation (D_{80}) against energy input at tip speeds of 5.23m/s, 6.54/s and 9.81m/s. The lower tip speed saves the specific energy 50–100 kWh/t. At each energy input point, the sample ground at tip speed 9.81 m/s produces most course product, and tip speed 6.54 m/s shows increased fineness. The lowest tip speed (5.23 m/s) gives the finest product. As energy input increases, the differences caused by varying the tip speed are slightly reduced. By setting the specific energy input as a target, lower tip speed takes longer time to input the same level of energy into the grinding chamber (shown in Table 1), but grinding efficiency is obviously improved. It saves about 25% specific energy input to obtain same fineness by grinding at tip speed 5.23 m/s compared to 9.81m/s. It indicates that lower tip speed may improve the grinding efficiency, but increase in time consumption normally is not desired in industrial applications.

Effect of grinding media

To evaluate the effect of the grinding media on the size reduction, the media Carbolite (sieve size +0.8 to -1.2mm, specific gravity 2.7 ± 0.1) and ZirPro (sieve size +0.7 to −1.4 mm, specific gravity 3.2 ± 01) were tested at three different tip speeds (5.23m/s, 6.54m/s and 9.81m/s). The media filling ratio and solids loading are kept at 52% (v/v) and 75% (w/w), respectively.

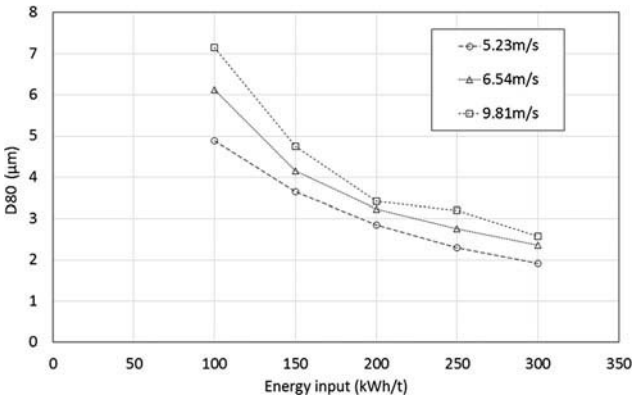

Figure 11. Details of the size variation against energy input by different tip speed.

Table 1. Time against energy input from different tip speed.

Specific energy (kWh/t)	V = 9.81 m/s time (min)	V = 7.85 m/s time (min)	V = 5.23 m/s time (min)
100	16	17	30
150	23	25	46
200	29	34	61
250	38	42	77
300	44	50	94

The D_{80} of the product size is compared in the Figure 12a–c. A stable and obvious difference is observed. The grinding media Carbolite demonstrates better grinding efficiency than ZirPro at all tested tip speeds. The most obvious advantage is obtained at tip speed 5.23 m/s shown in Figure 12a where at energy input 300 kWh/t, D_{80} obtained by Carbolite is 1.91 μm decreased by 1.81μm than product ground by ZirPro, D80 by which is 3.72 μm. Seen from Figure 12a–c, the average size gap is approximately 1 μm. Although this size difference may not be very huge, the difference on the amount of the energy required to obtain the improvement is significant. The energy efficiency is

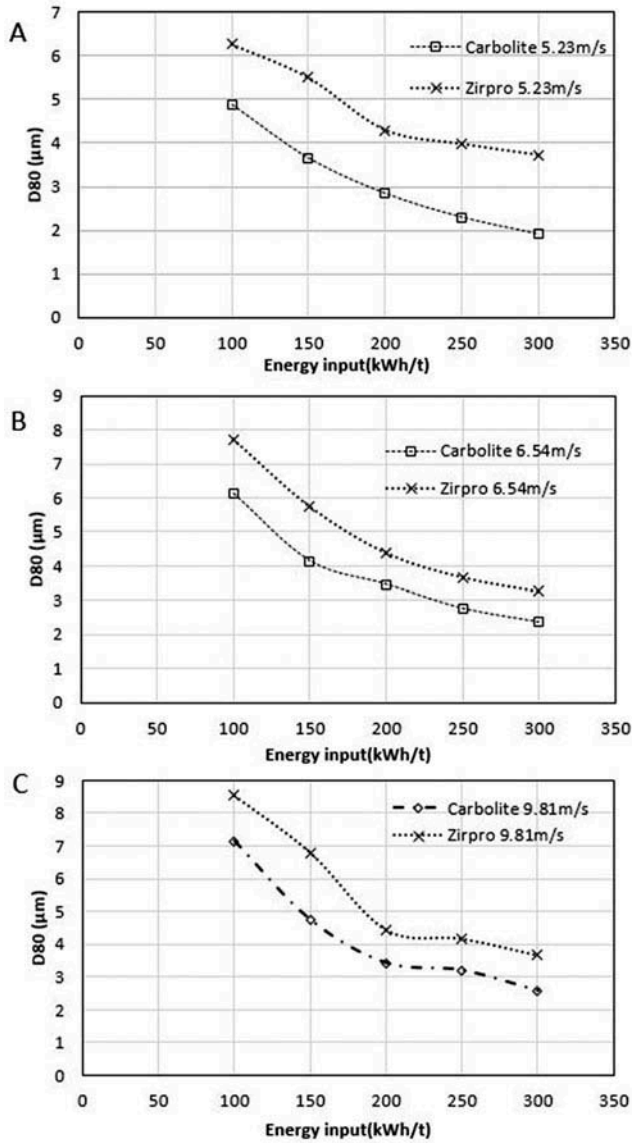

Figure 12. Comparison of the product size obtained by grinding media Carbolite and ZirPro at different tip speeds: (a) 5.23 m/s, (b) 6.54m/s and (c) 9.81m/s.

enhanced almost 40–50%. Some research pointed out that finer grinding bead produces finer size distribution.[24] As the sieve size of both grinding media is almost the same, it may not be the main reason. It is more likely contributed by the density of the Carbolite which is slightly lighter than the ZirPro and more close to the density of the calcium carbonate (2.7 g/cm^3), because a more homogeneous system is believed to be formed if the density of the grinding media is closed to the mineral.

Effect of impeller geometry

Some different configurations of impeller have been designed and tested to further investigate the grinding process. Figure 13 illustrates three types of impeller tested on a lab-scale mill. Type-A employs pitched flat blade instead of the pin stirrer. The pitched angle of the upper blade is designed to pump the slurry downward while the bottom blade could pump the slurry upward. Similar to type-A, type-B has an additional pin stirrer to fill the gap between upper and bottom blades. Type-C is configured by three parallel blades of which the cross-sectional shape is oval. The tip speed is fixed at 7.85 m/s with 65% solids loading with grinding media ZirPro (sieve size +0.7 to −1.4 mm, specific gravity 3.2 ± 01) at 52%(v/v) filling ratio. The velocity map is plotted according to PEPT data to illustrate the flow behavior of the charge.

Figure 14a displays velocity map by using type-A. It can be seen that the high speed area of the charge is mainly located in the gap between the impeller blades and wall of the chamber. Particularly in the field adjacent to the tip of the impeller blades, extremely the high velocity fields are observed with high media packing density. This phenomenon can be attributed to the distance of two impeller blades. Unlike the velocity map shown in Figure 10a–c, the motion of the charge depicted in Figure 14a is mainly located within the impeller band (height 0.04 − 0.1m).

Compared to the flow pattern obtained by impeller type-A (Fig. 14a), type-B (Fig. 14b) displays a centralised velocity field. By adding a pin stirrer with offset angel 90° to type-A, impeller type-B still provides sufficient space in the stirrer region to fluidise the charge; it holds the charge mostly in the central area. A notable

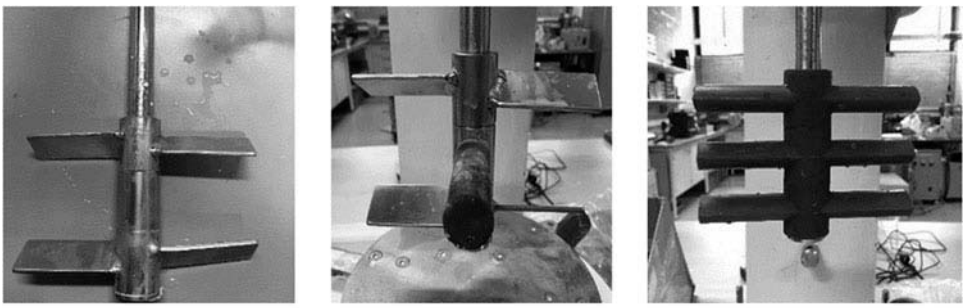

Figure 13. Photographs of tested impeller configuration (a) type-A, (b) type-B and (c) type-C.

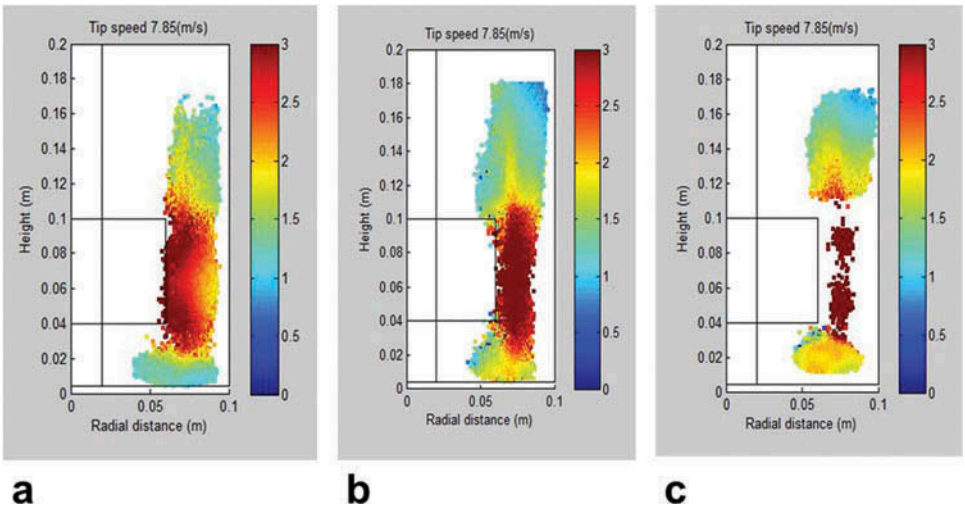

Figure 14. Velocity map plotted by impeller (a) type-A, (b) type-B and (c) type-C with grinding media ZirPro.

difference is that the height level of charge is increased. The charge is slightly squeezed away from the central area.

Figure 14c displays the flow behavior of the charge generated by impeller type-c. As the stirrer is mounted parallel with a relatively close distance, when a high tip speed is applied, it sweeps more like a solid blade. The narrow space between the two adjacent stirrer arms provides insufficient space for the charge to flow through. Also, very low packing density is observed near the impeller band. Undoubtedly, flow motion caused by type-c clearly is not desirable.

As the charge material is a high viscous slurry mixed with the grinding beads, it is difficult to disperse the slurry uniformly around the grinding chamber. By the increasing distance between the blades, it allows the slurry to flow across the stirrer surface with enough residence time to accelerate; otherwise, the charge is simply squeezed away without enough speed. If the kinetic energy is not sufficient for an effective breakage to occur, the energy might be simply wasted as heat.

Figure 15 displays the trend of size reduction using impeller type-A, type-B and type-C against specific energy input. Over energy input 100–300 kWh/t, D_{80} of product is reduced 1–2 μm by replacing standard impeller with new types of impeller. The finest product is obtained by type-A followed by type-B. Type-C demonstrates the lowest grinding efficiency at the same level of energy input. Optimization of the impeller design seems to be a promising and effective method to improve the grinding efficiency with no addition energy cost. Table 2 displays the time taken for each corresponding energy input. The type-C impeller shows a slight advantage over the type-A and type-B as it takes the shortest time to achieve

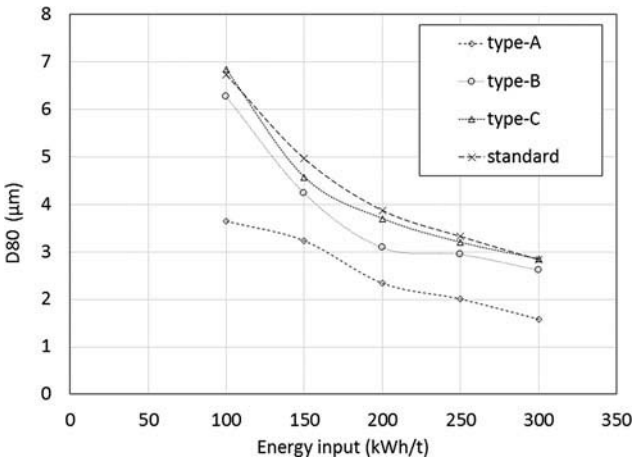

Figure 15. Details of size (D_{80}) against energy input from different impeller types.

Table 2. Time against energy input from different types of impeller.

Specific energy (kWh/t)	Type-A time (min)	Type-B time (min)	Type-C time (min)
100	15	14	13
150	21	25	20
200	27	36	26
250	34	46	32
300	40	56	38

the target energy input. This indicates that the type-C impeller consumes more energy in unit time than other two types, but it does not effectively transfer this energy to break particles. Most of the energy is probably dissipated as heat. Type-A undoubtedly is demonstrated as most efficient design compared to the other two types.

Conclusions

In this study, the effects of grinding operating parameters such as solids loading, tip speed and the design of the impeller were investigated. All the tests were conducted with a vertically stirred media mill. The effect of solids loading was tested at 65% and 75% solid concentration. The rheology data demonstrate that a higher viscosity is measured at a higher solids concentration. The slurry shows typical non-Newtonian behavior (shear thinning). Additionally, grinding performance data show the effect of solids concentration over size reduction. The lower solid loading proves to be more efficient for size reduction. The effect of tip speed has been studied at 5.23 m/s–9.81 m/s with velocity maps plotted by PEPT. Lower tip speed was found to be more suitable for the current operating conditions as a finer product is obtained. At the same tip speed range, comparison of the two types of grinding media is evaluated. The Carbolite is demonstrated to be more efficient than the ZirPro in the study. Finally, several different configurations of impeller have been analyzed to study the influence of the stirrer on grinding performance. Impeller type-A proves to have an advantage over other two types. The study also proves that optimization through altering the design of impeller is an effective and reliable way to realise the improvement of grinding efficiency.

Funding

The authors gratefully acknowledge Innovate UK and IMERYS for their financial support and technical help for this research.

References

[1] Altun, O., Benzer, H., Enderle, U. (2013) Effects of operating parameters on the efficiency of dry stirred milling. *Minerals Engineering*, 43–44:58–66.

[2] Radziszewski, P. (2013) Assessing the stirred mill design space. *Minerals Engineering*, 41: 9–16.

[3] Ouattara, S.; Frances, C. (2014) Grinding of calcite suspensions in a stirred media mill: Effect of operational parameters on the product quality and the specific energy. *Powder Technology*, 255: 89–97.

[4] Jankovic, A.; Valery, W.; Rosa, D.L., Fine grinding in the Australian mining industry. In 3rd International Conference on Recent Advances in Materials, Minerals and Environment (RAMM 2003), Malaysia, 2003.

[5] Xiao, X.; Zhang, G.; Feng, Q.; Xiao, S.; Huang, L.; Zhao, X.; Li, Z. (2012) The liberation effect of magnetite fine ground by vertical stirred mill and ball mill. *Minerals Engineering*, 34: 63–69.

[6] Shi, F.; Morrison, R.; Cervellin, A.; Burns, F.; Musa, F. (2009) Comparison of energy efficiency between ball mills and stirred mills in coarse grinding. *Minerals Engineering*, 22(7–8): 673–680.

[7] Kwade, A.; Schwedes, J. (2007) Chapter 6 wet grinding in stirred media mills. In: Salman, A.D., Ghadiri, M., Michael, J.H. (Eds.) *Handbook of Powder Technology*. Elsevier Science B.V. Amsterdam, Netherlands.

[8] Moore, P. (2012) Dust to dust-from primary crushing to ultrafine grinding, new comminution technology continues to give mines the edge in recovery and efficiency. *International Mining*, 56.

[9] Breitung-Faes, S., Kwade, A. (2013) Prediction of energy effective grinding conditions. *Minerals Engineering*, 43–44:36–43.

[10] Engstrom, J.; Wang, C.; Lai, C.; Sweeney, J. (2013) Introduction of a new scaling approach for particle size reduction in toothed rotor-stator wet mills. *International journal of pharmaceutics*, 456(2): 261–268.

[11] Altun, O.; Benzer, H.; Enderle, U. (2014) The effects of chamber diameter and stirrer design on dry horizontal stirred mill performance. *Minerals Engineering*, 69: 24–28.

[12] Jankovic, A.; Valery, W.; Davis, E. (2004) Cement grinding optimisation. *Minerals Engineering*, 17(11-12): 1075–1081.

[13] Jankovic, A.; Valery, W. (2013) Closed circuit ball mill – Basics revisited. *Minerals Engineering*, 43-44: 148–153.

[14] Bakalis, S.; Cox, P.W.; Russell, A.B.; Parker, D.J.; Fryer, P.J. (2006) Development and use of positron emitting particle tracking (PEPT) for velocity measurements in viscous fluids in pilot scale equipment. *Chemical Engineering Science*, 61(6): 1864–1877.

[15] Bakalis, S., Fryer, P.J., Parker, D.J. (2004) Measuring velocity distributions of viscous fluids using positron emission particle tracking (PEPT). *AIChE Journal*, 50 (7): 1606–1613.

[16] Barley, R.W.; Conway-Baker, J.; Pascoe, R.D.; Kostuch, J.; McLoughlin, B.; Parker, D.J. (2004) Measurement of the motion of grinding media in a vertically stirred mill using positron emission particle tracking (PEPT) Part II. *Minerals Engineering*, 17(11-12): 1179–1187.

[17] Conway-Baker, J.; Barley, R.W.; Williams, R.A.; Jia, X.; Kostuch, J.; McLoughlin, B.; Parker, D.J. (2002) Measurement of the motion of grinding media in a vertically stirred mill using positron emission particle tracking (PEPT). *Minerals Engineering*, 15: 53–59.

[18] Moys, M.H. (2015) Grinding to nano-sizes: Effect of media size and slurry viscosity. *Minerals Engineering*, 74: 64–67.

[19] He, M.; Wang, Y.; Forssberg, E. (2004) Slurry rheology in wet ultrafine grinding of industrial minerals: a review. *Powder Technology*, 147(1–3): 94–112.

[20] Bernhardt, C.; Reinsch, E.; Husemann, K. (1999) The influence of suspension properties on ultra-fine grinding in stirred ball mills. *Powder Technology*, 105: 357–361.

[21] Greenwood, R.; Rowson, N.; Kingman, S.; Brown, G. (2002) A new method for determining the optimum dispersant concentration in aqueous grinding. *Powder Technology*, 123: 199–207.

[22] Kwade, A. (2004) Mill selection and process optimization using a physical grinding model. *International Journal of Mineral Processing*, 74: 93–101.

[23] Becker, M.; Kwade, A.; Schwedes, J. (2001) Stress intensity in stirred media mills and its effect on specific energy requirement. *International Journal of Mineral Processing*, 61: 189–208.

[24] Jankovic, A. (2003) Variables affecting the fine grinding of minerals using stirred mills. *Minerals Engineering*, 16(4): 337–345.

[25] Tamblyn, R.J. (2005) Analysis of Energy Requirements in Stirred Media Mills; University of Birmingham

[26] Steffe, J.F. (1996) *Rheological Methods in Food Process Engineering*, 2nd Ed.; Freeman Press: East Lansing, MI, USA.